An experimental test for the mass independent isotopic fractionation mechanism proposed for ozone

François Robert, Lambert Baraut-Guinet, Pierre P. Cartigny, Peter Reinhardt

An experimental test for the mass independent isotopic fractionation mechanism proposed for ozone

François Robert[1], Lambert Baraut-Guinet[1,2], Pierre Cartigny[2], Peter Reinhardt[3]

[1]Institut de Minéralogie, Physique des Matériaux et Cosmochimie, UMR 7590, Muséum National d'Histoire Naturelle, 61 rue Buffon 75005 Paris

[2]Institut de Physique du Globe de Paris, 1 rue Jussieu 75005 Paris, France

[3]Laboratoire de Chimie Théorique, Sorbonne Université, 4 place Jussieu, 7525 Paris, France

Abstract

Ozone exhibits large and mass independent isotopic fractionations (MIF) in oxygen isotope ratios relative to molecular di-oxygen (O_2) from which it is formed. An interpretation of this effect was proposed based on the behavior of the indistinguishable isotopes ^{16}O in scattering processes. We report here an experiment aimed at testing one of the predictions of this model.

O_3 was formed by high frequency discharge in O_2 with pressures ranging between 1.6 and 38 Torr. The isotopic evolution of the closed O_2 reservoir was monitored during its distillation taking place during the continuous removal of ozone by condensation. Its composition evolves from a mass independent to a mass dependent fractionation along with the decrease in pressure. The isotopic pathways defined by this evolution in the 3 isotopes diagram are in quantitative agreement with the theoretical prediction of the disappearance of MIF with the increase of the complex lifetime stabilized as ozone.

Keywords

Ozone; Oxygen Isotopes; Mass Independent Fractionation; Experimental Observations; Theoretical Predictions.

Introduction

The discovery of a mass independent oxygen isotope fractionation (MIF) during the synthesis of ozone was found to contain a considerable potential for applications in Earth and Atmospheric Sciences[1-3]. A comprehensive set of experimental data illustrates this effect[4-16]. The origin of this physical phenomenon has been extensively discussed[17-29] but is still puzzling.

The isotopic composition of ozone is usually reported in relative variations expressed in per mil and noted in the $\delta^{m}O$ units:

$$\delta^{m}O = \{[(^{m}O/^{16}O)_{O_3} / (^{m}O/^{16}O)_{O_2}] -1 \} 1000 \quad (1)$$

with *m* standing for mass 17 or 18. Using these units, the isotopic compositions can be reported in a 3 isotopes diagram as $\delta^{17}O = f(\delta^{18}O)$ where quasi-linear correlations are defined by their slope *p*. For an infinite reservoir of O_2, the isotopic composition of the reservoir (i.e. $(^{m}O/^{16}O)_{O_2}$) remains constant during the synthesis of ozone. In this condition, $\delta^{m}O$ stands also for the overall isotopic fractionation factor ${}^{m}\alpha$ between O_2 and O_3:

$$\delta^{m}O = ({}^{m}\alpha -1) 1000 \quad (2)$$

The variations in the two isotope ratios $^{17}O/^{16}O$ and $^{18}O/^{16}O$ depend only on the difference in mass of the isotopes and, in this respect, are assumed to be *mass dependent*. In other terms, a change of 1‰ in $\delta^{17}O$ is accompanied by a change of ≈2‰ in $\delta^{18}O$; hence p=0.52[30-32]. Contrary to this theoretical and experimental prediction, the MIF effect observed during the synthesis of ozone yields p=1.0.

If the isotope fractionation results from two processes having a mass dependent and a mass independent isotopic fractionation factors, ${}^{m}\alpha_{,Mass\ Dep}$ and η respectively, the overall isotopic fractionation factor ${}^{m}\alpha$ can be expressed as:

$${}^{m}\alpha = {}^{m}\alpha_{,Mass\ Dep} \cdot \eta \quad (3)$$

with

$${}^{m}\alpha_{,\ Mass\ Dep.} = 1+\varepsilon(\alpha) \quad (4)$$

and

$$\eta = 1+ \varepsilon(\eta) \quad (5)$$

At this stage, in order to simplify the notations, we designate ^{16}O, ^{17}O and ^{18}O by 6, 7 and 8, respectively. Using this formalism, the variations of p in the 3-isotope diagram can then be understood as follows: when ozone is formed by a mass dependent process, ($|\varepsilon(\eta)| << |\varepsilon(\alpha)|$)

the isotopic compositions of O_3 are related by $p \approx 0.52$ and inversely, when ozone is formed purely by a mass independent process ($|\varepsilon(\eta)| >> |\varepsilon(\alpha)|$) $p \approx 1.00$.

The question raised by ozone can then be re-formulated such as: what is the physical origin of $\varepsilon(\eta)$[18] ? The solution of this question is complicated by the fact that the formation of ozone is a 3-body reaction and thus involves several reactions that yield isotopic selections. A simplified system describing the main reactions responsible for the formation of ozone is written as:

$O + O_2 \rightarrow O_3^*$ (k_f^*) (6)

$O_3^* \rightarrow O + O_2$ (k_D) (7)

$O_3^* + M \rightarrow O_3 + M$ (k_M) (8)

Reaction (6) describes the formation of the activated complex O_3^* (also referred to as metastable ozone) with the rate constant k_f^* (f for formation). Reaction (7) represents the spontaneous dissociation of the complex where the inverse of the rate constant k_D (D for dissociation) stands for the lifetime of the complex: $\tau = 1/k_D$. Reaction (8) corresponds to the possible stabilization of O_3^* by a third body M absorbing the proper amount of internal energy (the density of M is noted [M]). M can be a molecule of the gas phase or a solid surface.

At low pressure (P<1 Torr), $k_D >> [M].k_M$), the formation rate of ozone is written as:

$$d[O_3]/dt = [O].[O_2] \ \frac{k^*_f \ . \ k_M \ [M]}{k_D} \ = \ [O].[O_2] \ (k^*_f \ . k_M \ [M].\tau) \quad (9)$$

The isotopic fractionation factor ${}^m\alpha$ is the ratio of the rate constants k^*_f, $M.k_M$ and τ :

$${}^m\alpha \ = {}^mR_f \ x \ {}^mR_M \ x \ {}^mR_\tau \quad (10)$$

with ^{m}Rf, ^{m}RM and ^{m}Rτ standing for the k^*_f, $M.k_M$ and τ ratios involved in the formation of m66 and 666. Although no scientific consensus exists in the literature on the origin of the MIF effect[18-23,27,29], it has been proposed[33-34] that ^{m}Rf and ^{m}RM are mass dependent contrary to the lifetime ratios ^{m}Rτ of the different isotopomers of the complex: the lifetime τ would be different if the complex is formed by distinguishable (such as m+66) or by indistinguishable isotopes (such as 6+66)[33-34]. The channels accounting for isotope exchange and non-exchange between O and O_2 can be split when isotopes are distinguishable; but, this is not anymore possible when they are undistinguishable. As a consequence, the relative proportions of complexes formed by the exchange and non-exchange processes, cannot be calculated similarly when complexes formed via dis- or indistinguishable isotopes. Their average lifetime τ is thus different. This effect takes place during the scattering of oxygen atoms by O_2 and is independent of the interaction potential between O and O_2. In other terms, MIF does not result from an

isotope-exchange reaction, but reflects the isotopic composition of the fraction of the activated complexes that is sampled through their stabilization as ozone (reaction 8). The lifetime ratio ${}^{m}R_{\tau}$ is ascribed to the mass independent isotopic fractionation factor and is noted ${}^{m}\eta$[19].

${}^{m}\eta$ has been modeled numerically in classical mechanics[33], assuming that the quantum terms are negligible when rates are averaged in a thermal situation. This assumption has been numerically verified by[35]. Several numerical predictions arising from these calculations are specific to this theory and can be used for practical purposes. In this paper, we report an experiment dedicated to test one of these predictions, namely: ${}^{m}\eta$ should vary with the lifetime of the complex hence with the pressure of the bath.

In the laboratory, ozone (O_3) produced in a molecular oxygen plasma by electric or microwave discharge or by O_2 photolysis, is condensed on the glass walls of the apparatus at liquid nitrogen temperature. At O_2 pressures <10 Torr, a progressive transition has been observed[6, 9, 10, 16] between the two regimes of isotopic fractionation i.e. with p varying between 1.0 and 0.52 during the decrease in pressure. In addition, when p=1.0 or p=0.52 ozone is either enriched or depleted in the heavy isotopes, respectively. This effect was interpreted as the progressive transition between two distinct processes: a homogeneous (mass independent; p=1.0) and a heterogeneous (mass dependent; p=0.5) reaction taking place on the walls of the apparatus [6, 9, 10, 16].

Bains-Sahota and Thiemens[6] ascribed this low pressure reaction to the formation of O_2 by the recombination of two oxygen atoms while Janssen and Tuzson[14] called upon the fast isotopic equilibrium between O and O_2:

$$m + 66 \leftrightarrow 6 + m6 \qquad (11)$$

Ozone being formed by the reaction between oxygen atoms and O_2 from the bath, the isotopic composition of ozone would reflect the isotopic composition of the oxygen atoms in (11). Since the equilibrium reaction (11) is much faster that the stabilization rate of the complex, Janssen and Tuzson[14] have proposed that the reverse reaction (7) overcomes the stabilization reaction (8). However, observations[15] and theoretical considerations clearly indicate that the complex states reached isotopic equilibrium with the reactants in the gas phase at pressures well above 10 Torr, i.e. well above the domain in pressure where the progressive change of p is observed. Therefore, the theoretical origin of the p variations remains an open question.

We have studied the evolution of p for a finite reservoir of O_2 where the isotopic composition of O_2 changes along with the removal of O_3 and with the change in pressure.

Based on these new results and using the theoretical prediction according to which ${}^{m}\eta$ is pressure dependent, we show that another interpretation is possible to account for the change of p at low pressure.

1. Experimental methods

Ozone is produced by a high-frequency discharge in natural oxygen (research grade purity) and is continuously removed from the bath through its condensation on the glass walls of the apparatus at liquid N_2 temperature. The oxygen gas is introduced in the reactor (about 3700 cm^3, cylinder-like shape with 5cm radius and 40cm length) through a Pyrex tube (Figure 1). The isotopic composition of O_2 is recorded as pressure steps i.e. when the reaction stops, the pressure of the remaining O_2 is measured and a small aliquot of O_2 is sampled and isotopically analyzed. The evolution of pressure is monitored by a piezo-sensitive gauge Pfeiffer APR26.

Eight sets of experiments are run with initial pressure of 5.39, 10.33, 10.43, 11.45, 18.05, 26.52, 30.16 and 37.56 mbar respectively (see table 1). A radio frequency high voltage discharge is applied manually with a Tesla coil on one single metallic electrode (inox-made) located at the center of the Pyrex cylinder tube. A glow discharge is visible at the lowermost part of the electrode, where small light sparks can be seen. The lower part of the reactor, about 60% in volume, is immerged in liquid nitrogen (~87 K).

The reaction and the mass spectrometric analyses are made through the following successive operations (cf. Figure 1): (i) the reactor is outgassed by opening the stopcocks (1) and (3) and similarly, for the admission of O_2 in the reactor, (ii) the stopcock (3) is closed and the upper volume (20 cm^3) limited by the 3 stopcocks is continuously pumped out, (iii) when the discharge is stopped, the stopcock (1) is closed and an aliquot of O_2 is sampled by opening the stopcock (3) (ozone remaining trapped cryogenically on the reactor walls), (iv) after 30 sec. for pressure equilibration, the stopcock (3) is closed and an aliquot of O_2 is injected in a Dual-Inlet Isotopic Ratio Mass-Spectrometer (DI-IRMS; see Figure 1) by opening the stopcock (2). This last operation yields a decrease of the pressure in the reaction vessel of the order of a few %.

The isotopic composition is measured with a mass spectrometer ThermoFischer Delta V DI-IR-MS. The analytical precision (1 std. dev.) on isotopic analyses is ±0.082 and ±0.040 ‰, for $\delta^{17}O$ and $\delta^{18}O$, respectively. The mass resolution of the instrument is ≈150 ($\Delta m/m$). The amount of analyzed gas lies between 10 and 80 μmole STP.

2. Results

Results are reported in Table 1 and 5 experiments out of 8 are reported in Figure 2. O_2 was introduced in the reaction vessel at an initial pressure Pi. In the Janssen and Tuzson experiment[14] the amount of synthetized O_3 did not cause a noticeable change in the O_2 pressure and thus, the isotopic fractionation factor ${}^{m}\alpha$ was directly accessible by measuring $\delta^{17}O$ and $\delta^{18}O$ in O_3. In contrast to this, the present experiment lead to a reservoir effect (hereafter referred to as a "*distillation*") where the pressure and the isotopic compositions of O_2 diminish along with of the condensation of O_3. The duration of the reaction, the initial and final pressures Pi and Pf are also reported in Table 1 for each step.

The evolution of the $\delta^{18}O$ with pressure is reported in the Figure 2. In this figure, the pressure stands for the average value between Pi and Pf except for the first step where the pressure is the initial Pi value. The $\delta^{18}O$ shows first a decrease in the first pressure steps, followed by an increase for the last fractions of the remaining O_2 reservoir. During the decrease in pressure, the $\delta^{18}O$'s go through minimum values which occur at different pressures among the experiments, depending on the initial pressure of the O_2 reservoir. This minimum value corresponds to a 45-55% decrease in pressure relative to the initial pressure value.

The evolutions of the isotopic compositions of O_2 caused by the removal of O_3 are also reported as pathways in the 3 isotopes diagram (Figure 3). In several experiments, $\delta^{17}O$ and $\delta^{18}O$ show first a decrease along a slope $p\approx1.0$ followed by an increase along a slope $1>p>0.5$. The correlation slope p varies between ≈1.0 and ≈0.52 i.e. between a pure mass independent and a pure mass dependent fractionation.

Note that $p=0.71$ is usually observed when the discharge takes place between two electrodes[6,10,13-14]. We have also reproduced experimentally $p=0.71$ by using an electric discharge between two electrodes[36]. This departure of p from unity would reflect a mass dependent isotope fractionation occurring either during the dissociation of O_3 by electron impact in the discharge or by a simple thermal dissociation of O_3. In these conditions, ozone results from a two steps process: a formation mechanism along the slope 1.00 and a dissociation mechanism along the slope 0.52; hence a resulting slope of 0.71. In the course of this study, it has been verified that the slope p is exactly equal to 1.0 for a O_2 pressure around 80 Torr and when using a single electrode to promote the discharge. Therefore, this dissociation mechanism is not taking place in the present experiment.

As shown in this Figure, $\delta^{17}O$ and $\delta^{18}O$ in the remaining O_2 becomes progressively depleted in $^{17,18}O$ when the pressure diminishes indicating that ozone is enriched in $^{17,18}O$ and lies on a slope $p=1.0$. The shift of slopes at low pressures from $p=1.0$ to $p\approx0.52$ is associated with an

increase in $\delta^{17}O$ and $\delta^{18}O$ in the remaining O_2 ($p \approx 0.5$; Sample #1), indicating that ozone is now depleted in $^{17,18}O$ in a mass dependent manner. Such a behavior is usually referred to as a *cross-over* in the isotopic fractionation factor.

This *cross over* is qualitatively in agreement with previous observations[6,14]. It was interpreted[14] as an evolution in the relative contributions of

(i) ozone formed in the gas phase reaction with $p \approx 0.71$ corresponding to the maximum $\delta^{17}O$ and $\delta^{18}O$ values in O_3 equal to +110‰ and +140‰, respectively and of

(ii) ozone formed on the glass walls by the reaction (11) with $p \approx 0.52$ ($\delta^{18}O$ values in O_3 around −35‰).

In other terms, the change in the ozone isotopic composition would result from the evolution of the relative proportions of ozone formed by two types of chemical reactions. However, in Figure 3, it can be observed that the linear relations of the isotopic evolutions toward positive $\delta^{17}O$ and $\delta^{18}O$ values do not converge toward a unique composition that would stand for the component (ii).

As a summary, these new results are difficult to reconcile with a two end-member mixing model. They are compared in the next session with the predicted theoretical relation between ${}^{m}\alpha$ and the lifetime of the complex

3. Interpretation

The present interpretation is based on the formalism developed by Reinhardt et Robert[33,34]. Our purpose here is not to perform a complete physical treatment of oxygen chemistry in the plasma. Numerical simplifications can be made in the calculation of the isotopic fractionation ${}^{m}\alpha$ if one considers only the ratio of isotopically substituted reaction rate constants[32]. Indeed, in most cases, the interaction potentials are not affected by the isotopic substitution and such ratios (as ${}^{m}R_f$ or ${}^{m}R_M$ in (10)) can be supposed to be mass dependent. This assumption is still theoretically investigated in great details[37, 38].

In[34], a simple model for the stabilization of the complex has been assumed: ozone would be stabilized above the minimum lifetime value τ_{Min}. Below τ_{Min}, the complex spontaneously dissociates and O_2 returns to the gas phase via reaction (7). The relation between the weighted average lifetime $\overline{\tau}$ and τ_{Min} has been computed and is reported in Figure 4 (see[34] for details). In this Figure, the difference between ${}^{17}\overline{\tau}$ and ${}^{18}\overline{\tau}$ being negligible, m has been omitted in $\overline{\tau}$ for simplicity. In the rest of the paper we will use $\overline{\tau}$ in place of τ_{Min}, $\overline{\tau}$ being an intensive parameter of the reaction forming ozone.

Considering only the natural isotopic abundances of oxygen (i.e. $8/6 \approx 2 \times 10^{-3}$ and $7/6 \approx 4 \times 10^{-4}$), the 3 isotopomers 666 and m66 are the most abundant species. The 4 atom-molecule reactions producing the scrambled products $^{m}O^{16}O^{16}O^{*}$ are restricted to:

$$m + 66 \rightarrow m66^{*} \quad (12)$$

$$6 + m6 \rightarrow 6m6^{*} \quad (13)$$

$$6 + 6m \rightarrow 66m^{*} \quad (14)$$

In italic, the knock-on atom of the molecule O_2. Reaction (12) stands for the two reactions between m and 6. Note that reactions (12) and (14) correspond to the forward and backward reaction (11) for isotope exchange. The atom-molecule reactions producing $^{16}O^{16}O^{16}O^{*}$ is:

$$6 + 66 \rightarrow 666^{*} \quad (15)$$

The lifetime for the reaction (15) is noted $\overline{\tau}_I$ with the subscript I for indistinguishable.

We define the lifetime ratio as the mass independent isotopic fractionation factor η:

$$\eta(\overline{\tau}) = \overline{\tau} / \overline{\tau}_I \quad (16)$$

Experimental data and numerical simulations[13,39,40] reveal that both mass dependent and mass independent isotopic mass fractionation takes place in the stabilization rate of O_3^{*} at the low pressure regime. For example, the average lifetime of the 666 complex is shorter than the lifetime of 688 but longer than the lifetime of 866[39]. This mass dependent effect is theoretically well understood and involves the quantum mechanical differences in the vibrational zero-point energies (ΔZPE) between entrance and exit channels in the $O+O_2$ reaction[13,39,40].

This vibrational contribution (noted ν) is related to the difference in the ΔZPE between the reactants ($O+O_2$) and the products (O_3) and has been experimentally measured by[13] for several isotopomers of ozone. In the case of the natural abundances of ^{17}O and ^{18}O, each reaction (12), (13) and (14) contributes for $1/3$ in the overall isotopic fractionation factor[33]. This gives the mass independent isotopic fractionation factor $^{m}\eta(\overline{\tau})$ (i.e. the overall lifetime ratio)[34]:

$$^{m}\eta(\overline{\tau}) = 1/3\,[\eta(\overline{\tau}).{}^{m}\nu_{12}] + 1/3\,[\eta(\overline{\tau}).{}^{m}\nu_{13}] + 1/3\,[\eta(\overline{\tau}).{}^{m}\nu_{14}] \quad (17)$$

with the subscripts standing for the reactions (12), (13) and (14). The computed numerical ν values are[34]:

$$^{17}\nu_{12} = 0.867; \quad ^{17}\nu_{13} = 1.000\ (\Delta ZPE=0); \quad ^{17}\nu_{14} = 1.133 \quad (18)$$

$$^{18}\nu_{12} = 0.746; \quad ^{18}\nu_{13} = 1.000\ (\Delta ZPE=0); \quad ^{18}\nu_{14} = 1.254 \quad (19)$$

Note that the masses of the isotopes for the translation and rotation movements were also considered in the calculations of $\eta(\overline{\tau})$[33]; these mass corrections are negligible and are not mentioned here for simplicity. Numerical results for $^{17}\eta(\overline{\tau})$ and $^{18}\eta(\overline{\tau})$ as a function of $\overline{\tau}$ are

reported in Figure 5. They exhibit a maximum around $\overline{\tau} \approx 30$ ps which is in agreement with the maximum isotopic fractionation experimentally observed in ozone and in agreement with experimental determinations for $\overline{\tau}$[42]. This gives at $\overline{\tau} \approx 30$ ps, $^{17}\eta(\overline{\tau}) = 1.114$ and $^{18}\eta(\overline{\tau}) = 1.116$, giving $p=1$ in the three isotopes diagram.

In the gas phase, $\overline{\tau}$ is constant and leads to the third order reaction (9). As a consequence, the ratio $\delta^{17}O/\delta^{18}O$ exhibits a plateau at pressure P≲100 Torr. However, if ozone is produced on the walls of the apparatus, the reaction should not depend anymore on the density of the third body [M] and the reaction (9) becomes second order. This situation is achieved if one supposes that $\overline{\tau}$ varies as P^{-1} on the walls.

Looking now at Figure 5, it can be noted that $\eta(\overline{\tau})$ varies rapidly with $\overline{\tau}$. As shown in Figure 5, $\eta(\overline{\tau}) \rightarrow \approx 1$ when $\overline{\tau} \rightarrow \infty$. $\overline{\tau}$ can be related inversely to the pressure, as the occurrence of the two possible reactions (O_3* with the wall at an average time constant and O_3* in the gas stabilized by the encounter with M) tend to favor the reaction with the walls when the pressure diminishes. The average lifetime before a stabilizing collision will thus be shorter at high pressure than at low pressure (and, of course shorter than for a case without walls). Therefore, we assume that $\overline{\tau}$ is inversely proportional to pressure.

$$\overline{\tau} \propto P^{-1} \tag{20}$$

This hypothesis has two consequences: when the pressure diminishes (i) the reactions (9) should becomes progressively second order and (ii) since $\eta(\overline{\tau}) \rightarrow \approx 1$, the mass independent effect should disappear. This is in qualitative agreement with several observations reported in the literature[6,9,10,14] where the decrease in $\delta^{17}O$-$\delta^{18}O$ was observed below ≲30 Torr and ascribed to wall effects. Ascribing this effect to a change in the lifetime of the complex stabilized as ozone, the observed pathways in the $\delta^{17}O$-$\delta^{18}O$ diagram can be simulated numerically.

We define ^{m}f as the isotope exchange equilibrium constant of the reactions (12) and (14) (m+66 and 6+6m):

$$^{m}f = (^{m}O/^{16}O)_O / (^{m}O/^{16}O)_{O_2} \tag{21}$$

The term ^{m}f was not considered in our previous theoretical approach[34] that was focused on the numerical evaluation - and origin - of the mass independent fractionation factor $^{m}\eta(\overline{\tau})$. In the present experiment where all isotopomers are scrambled, the overall isotopic fractionation factor $^{m}\alpha(\overline{\tau})$ becomes:

$$^{m}\alpha(\overline{\tau}) = {}^{m}f \,.\, {}^{m}\eta(\overline{\tau}) \tag{22}$$

Note that ${}^{m}f<1$ while ${}^{m}\eta(\overline{\tau})>1$ i.e. are of opposite signs in δ units. Consequently, when the mass independent isotopic effect becomes negligible (i.e. ${}^{m}\eta(\overline{\tau})\approx 1$), ozone should be depleted in $^{17,18}O$ relative to O_2 with $p\approx 0.5$ while, when ${}^{m}\eta(\overline{\tau}) > {}^{m}f$, ozone should be enriched in $^{17,18}O$ relative to O_2 with $p\approx 1$. In the following calculations, we use the measured[14] (and calculated[43]) values for f: ${}^{18}f=0.965$ (i.e. $\delta^{18}O= -35‰$) and ${}^{17}f=0.982$ (i.e. $\delta^{17}O= -18‰$).

The isotopic fractionation of oxygen isotopes during the distillation of O_2 via the condensation of O_3 can be written as:

$$d[{}^{m}O] / d[{}^{16}O] = {}^{m}\alpha({}^{[16}O]) \cdot \{[{}^{m}O]/[{}^{16}O]\} \quad (23)$$

with ${}^{m}\alpha({}^{[16}O])$ being a function of the overall pressure:

$${}^{m}\alpha({}^{[16}O]) \propto {}^{m}\alpha(P^{-1})) \propto {}^{m}\alpha(\overline{\tau})) \quad (24)$$

When ${}^{m}\alpha$ is constant, equation (23) yields the so-called Rayleigh equation. Using the variations ${}^{m}\alpha(\overline{\tau})$ reported in the Figure 5, the equation (23) has been solved numerically by adjusting $\tau=30$ ps for $P=30$ Torr. Results for $\delta^{17}O$ and $\delta^{18}O$ are reported in Figure 6. They reproduce the data with no additional free parameter. For the sake of clarity, the present calculation is still a first order approximation since the measured isotopic values stand for the function (23) integrated between the initial and final pressure of each step. We neglect this refinement.

Note that f values vary with the temperature of the bath. This temperature is difficult to estimate since there is a strong temperature gradient between the center of the plasma and the walls at Liq. N_2 temperature. However, as long as $(1- {}^{17}f).1000 = 0.52\ (1- {}^{18}f).1000$ (i.e. ${}^{17}f$ mass dependently related to ${}^{18}f$), the numerical simulation is (almost) insensitive to f values for $0.94<{}^{18}f<0.98$.

In experimental literature[6, 9, 14], the O_2 reservoir is infinite i.e. O_2 is continuously renewed in the reaction chamber. In such condition the mixing ratio between ozone formed in the gas phase and on the walls cannot be constrained by a distillation model but by the reaction rate ratio between ozone formed on the walls and formed in the gas. As shown by Morton et al.[9], the evolution of $\delta^{17}O/\delta^{18}O$ with the pressure depends also on the size of the reservoir, demonstrating the role of the walls in the overall production rate of ozone. In agreement with the present results, Morton et al.[9] reported, for a volume of reaction (volume 35 mL, r≈5cm) similar to the present experiment, a change in p beginning around 30 Torr.

However, in conditions of an infinite reservoir, the evolution of ozone with pressure defines straight lines in the $\delta^{17}O/\delta^{18}O$ diagram compatible with a two end-member mixing model i.e. with ozone formed on the walls ($p=0.52$) resulting from a different reaction than ozone formed

in the gas (p=1.0). This property of the evolution of the ozone $\delta^{17}O/\delta^{18}O$ has been observed in all previously reported experiments[6, 9, 14]. The change in η with the lifetime of the complex as reported in Figure 5, should also define a straight line in the $\delta^{18}O$-$\delta^{17}O$ diagram. Therefore, for experiments performed with an infinite reservoir of O_2, it is impossible to decide if the evolution of the isotopic composition of ozone in the $\delta^{18}O$-$\delta^{17}O$ diagram should be ascribed to η or to the evolution of the mixing ratio of ozone produced by two different reactions (in the gas and on the walls).

As mentioned previously, a cross over in the $\delta^{17}O$-$\delta^{18}O$ distillation pathway can also be predicted by previous experimental results[6,14]. We have therefore performed a similar distillation calculation with constant isotopic fractionation factors (i.e ${}^{m}\alpha(\overline{\tau})$ and ${}^{m}f$). Contrary to the assumption where ${}^{m}\alpha(\overline{\tau})$ changes with the lifetime of the complex, these conditions do not reproduce the pathways defined by the present data.

The present observations confirm that glass walls trigger the stabilization of the complex but the numerical treatment of the distillation does not call upon other formation reactions than those involved in the gas phase (eq. 9). In other terms, the change in sign in the $\delta^{17}O/\delta^{18}O$ values is not caused by the evolution of the mixing ratio between two ozone species but by the evolution of the overall isotopic fractionation factor. The stabilization on the walls yields a selection in the lifetime distribution of the complex.

This interpretation raised one issue: the transition between the two regimes of stabilization of the complex $[O_3]^*$ should theoretically occur around 10^{-2} Torr and not around 10 Torr as postulated here. This argument is also reinforced experimentally: in an afterglow of pulsed discharges[44], it has been shown that the O_3 surface production rate depends on the density of adsorbed O and O_2 on solid surfaces and consequently, that ozone produced on the walls in the range 1-5 Torr should not contribute significantly to its overall production. This point remains an open issue.

Conclusions

The isotopic variations in $\delta^{17}O/\delta^{18}O$ observed experimentally during the condensation of ozone in a close reservoir of O_2, are in agreement with variations with pressure of the mass independent isotopic fractionation factor η[34]. The cross over in the isotopic evolution of the remaining reservoir would not be caused by an additional reaction forming ozone but would be intrinsic to the overall isotopic fractionation factor.

In this model, the "*anomalous*" isotopic effect is not restricted to the formation of ozone nor to oxygen isotopes. If correct, this opens a wide range of possible applications to experimental or natural systems for other chemical elements.

Acknowledgements

This work has been founded by the ERC Advanced Grant *PaleoNanoLife* (PI: F. Robert; 161764). We wish to thank Mark Thiemens, Dmitry Babikov, Fabien Gatti and Christof Janssen for their time in long debates. We also thank Guillaume Lombardi and Karim Hassouni for their expertise in plasma physics

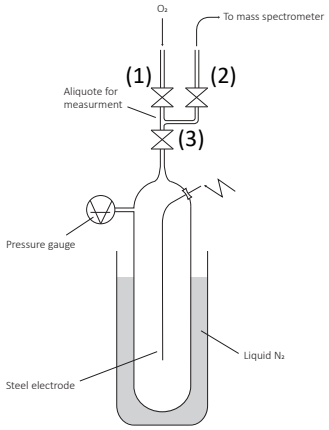

Figure 1: Oxygen discharge experiment. After condensation of ozone at liquid nitrogen temperature on the walls of the vessel, an aliquot of the remaining O_2 is sampled via the *Aliquot* set up and send directly to the mass spectrometer (see Experimental).

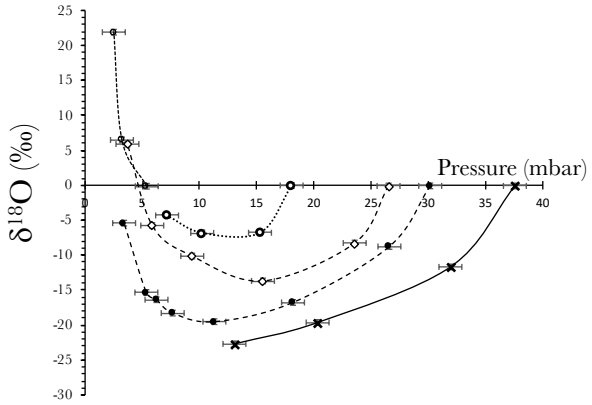

Figure 2: The isotopic composition ($\delta^{18}O$) of molecular oxygen is reported as a function of Pressure. Note that the minimum $\delta^{18}O$ values is reached at different pressure and is related to the initial pressure.

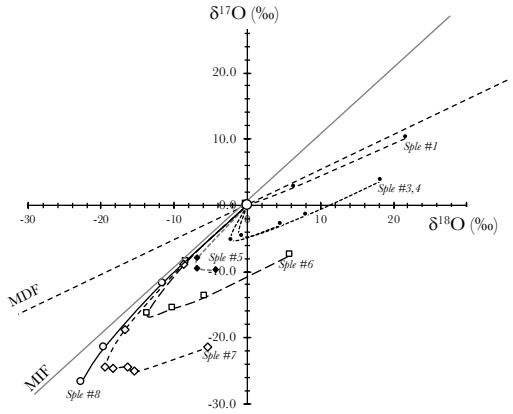

Figure 3: The isotopic compositions of O_2 are reported in the 3 isotopes diagram in δ^mO units (data in Table 1). They define distillation pathways caused by the continuous removal of O_3 by its condensation at liquid nitrogen temperature on the walls of the vessel. The evolution of these pathways depends on the initial pressure of O_2. The mass dependent ($p=0.52$) and mass independent ($p=1$) fractionation lines are shown for references. Note that the pathways do not define converging linear correlations.

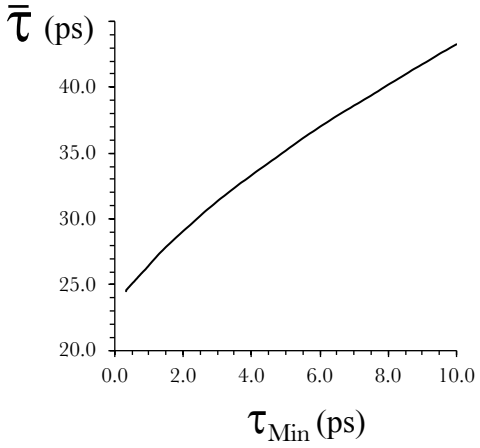

Figure 4: The relation between the weighted average lifetime $\overline{\tau}$ and the minimum lifetime τ_{Min}. The difference between ${}^{17}\overline{\tau}$ and ${}^{18}\overline{\tau}$ being negligible at this scale, has been omitted.

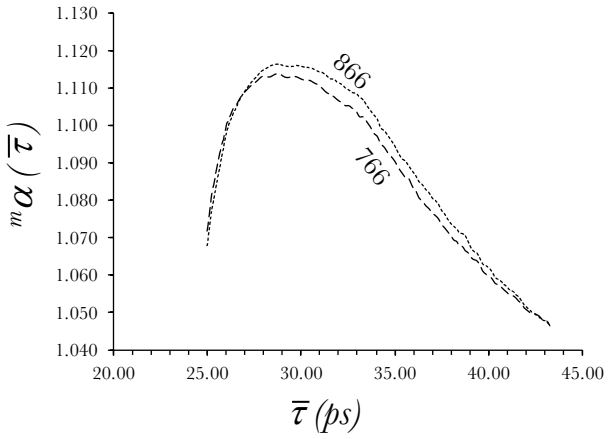

Figure 5: The mass independent isotopic fraction factors $^{m}\eta(\tau) = (^{m}O/^{16}O)_{O3} / (^{m}O/^{16}O)_{O2}$ with m standing for mass 17 or 18 (cf. equation (17)) are reported as a function of the average lifetime $\overline{\tau}$ of the complex O_3*. The notations 6, 7 and 8 stand for ^{16}O, ^{17}O and ^{18}O. $^{m}\eta(\tau)$ is calculated for a scrambled mixing of the isotopomers 6-6m, 6-m-6 and m-66.

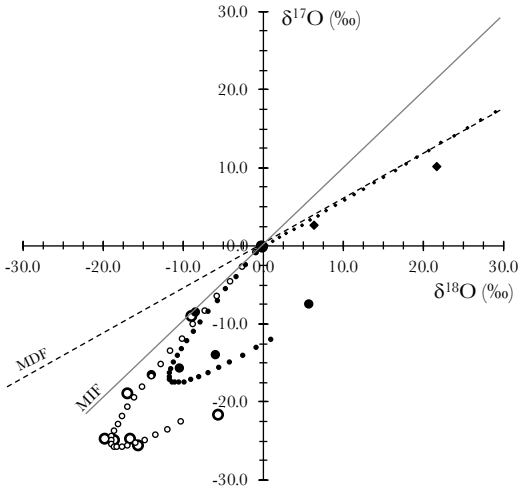

Figure 6. The computed isotopic compositions of O_2 in a distillation model are reported in the 3 oxygen isotopes diagram. The mass dependent (MDF) and mass independent fractionation (MIF) lines are shown as references. For comparison with experimental data, the dot symbols are used for calculated values while larger symbols are used for experimental data.

Sample	Duration (min)	ΔPressure (Torr)	$\delta^{17}O$(‰)	$\delta^{18}O$(‰)
#1,0	0	5.39	-0.08 ± 0.08	-0.14 ± 0.02
#1,1	15	5.39, n.m.	2.73 ± 0.11	6.48 ± 0.05
#1,2	30	3.22, 1.80	10.20 ± 0.21	21.89 ± 0.05
#2,0	0	10.43	-0.08 ± 0.08	-0.14 ± 0.02
#2,1	24	10.43, 6.5	-2.32 ± 0.05	2.25 ± 0.04
#2,2	37	4.13, 2.58	-1.29 ± 0.16	4.43 ± 0.09
#3,0	0	10.33	-0.08 ± 0.08	-0.14 ± 0.02
#3,1	22	10.33, 5.83	-4.79 ± 0.07	-0.64 ± 0.04
#3,2	37	4.9, 2.56	-1.48 ± 0.14	8.17 ± 0.05
#3,3	48	2.06, 1.65	3.72 ± 0.09	18.41 ± 0.09
#4,0	0	11.45	-0.08 ± 0.10	-0.12 ± 0.02
#4,1	24	11.45, 6.30	-5.28 ± 0.08	-2.08 ± 0.03
#4,2	47	5.05, 3.75	-3.00 ± 0.06	4.68 ± 0.04
#5,0	0	18.05	-0.03 ± 0.05	-0.04 ± 0.03
#5,1	22	18.05, 12.52	-7.96 ± 0.05	-6.79 ± 0.01
#5,2	35	11.26, 9.21	-9.51 ± 0.04	-6.81 ± 0.03
#5,3	51	8.50, 5.83	-9.83 ± 0.06	-4.32 ± 0.03
#6,0	0	n.m.	-0.02 ± 0.08	-0.11 ± 0.30
#6,1	19	26.52, 20.60	-8.51 ± 0.08	-8.27 ± 0.03
#6,2	44	19.1, 11.99	-16.44 ± 0.03	-13.69 ± 0.03
#6,3	68	10-79, 7.94	-15.59 ± 0.08	-10.13 ± 0.04
#6,4	80	6.77, 4.97	-13.88 ± 0.13	-5.76 ± 0.03
#6,5	97	4.14, 3.26	-7.57 ± 0.07	5.90 ± 0.04
#7,0	0	n.m.	-0.02 ± 0.09	-0.09 ± 0.03
#7,1	19	30.16, 23.03	-8.93 ± 0.06	-8.76 ± 0.04
#7,2	44	21.49, 14.85	-18.80 ± 0.06	-16.77 ± 0.02
#7,3	70	13.60, 9.01	-24.45 ± 0.04	-19.51 ± 0.03
#7,4	80	8.18, 7.13	-24.60 ± 0.10	-18.28 ± 0.02
#7,5	87	6.36, 6.12	-24.41 ± 0.07	-16.37 ± 0.02
#7,6	95	5.51, 5.20	-25.19 ± 0.07	-15.35 ± 0.01
#7,7	117	4.36, 2.46	-21.49 ± 0.02	-5.42 ± 0.03
#8,0	0	37.56	-0.07 ± 0.05	-0.10 ± 0.01
#8,1	28	37.56, 26.29	-11.85 ± 0.10	-11.68 ± 0.04
#8,2	57	23.92, 16.72	-21.56 ± 0.06	-19.63 ± 0.04
#8,3	73	15.03, 11.05	-26.67 ± 0.15	-22.69 ± 0.03

Table 1: In the successive columns, are reported: The samples in their chronological sampling order, the duration of the discharge, the pressure variation of the O_2 reservoir and the isotopic compositions of the remaining O_2 expressed in $\delta^{m}O$ (‰) units. (n.m. for not measured).

References.

(1) Thiemens, M.H.; Heidenreich, J.E. The mass-independent fractionation of oxygen - a novel isotope effect and its possible cosmochemical implications. *Science* **1983**, *219*, 1073-1075.

(2) Thiemens, M.H. Atmosphere science - Mass-independent isotope effects in planetary atmospheres and the early solar system. *Science* **1999**, *283*, 341-345.

(3) Thiemens M.H. Introduction to Chemistry and Applications in Nature of Mass Indepedendent Isotope Effects Special Feature. **2013**, 110, 44, 17631-17637. doi.org/10.1073/pnas.1312926110

(4) Thiemens, M.H.; Gupta, S.; Chang, S. The observation of mass-independent fractionation of oxygen in an RF discharge. *Meteoritics 18*, **1983**, 408-409.

(5) Heidenreich III, J.E.; Thiemens, M.H. A non-mass-dependent oxygen isotope effect in the production of ozone from molecular oxygen – the role of molecular symmetry in isotope chemistry. *J Chem Phys* **1986**, *84*(4): 2129–2136.

(6) Bains-Sahota, S.K.; Thiemens M.H. Mass-Independent Oxygen Isotopic Fractionation in a Microwave Plasma. *J. Phys. Chem.* **1987**, *91*, 4370-4373.

(7) Anderson, S.M.; Morton, J.; Mauersberger, K. Laboratory measurements of ozone isotopomers by tunable diode-laser absorption-spectroscopy. *Chemical Physics Letters* **1989,** *156*, 175-180.

(8) Morton, J.; Schueler, B.; Mauersberger, K. Oxygen fractionation of ozone isotopes O-48 through O-54. *Chemical Physics Letters* **1989**, *154*, 143-145.

(9) Morton, J.; Barnes, J.; Schueler, B.; Mauersberger, K. Laboratory studies of heavy ozone. *Journal of Geophysical Research-Atmospheres* **1990**, *95*, 901-907.

(10) Thiemens, M.H.; Jackson, T. Pressure dependency for heavy isotope enhancement in ozone formation. *Geophys. Res. Lett* **1990**, *17*, 717-719.

(11) Mauersberger, K.; Morton, J.; Schueler, B.; Stehr, J.; Anderson, S.M. Multi-isotope study of ozone - implications for the heavy ozone anomaly. *Geophysical Research Letters* **1993**, *20*, 1031-1034.

(12) Mauersberger, K.; Erbacher, B.; Krankowsky, D.; Gunther, J.; Nickel, R. Ozone isotope enrichment: Isotopomer-specific rate coefficients. *Science* **1999**, *283*, 370-372.

(13) Janssen, C.; Guenther, J.; Mauersberger, K.; Krankowsky, D. Kinetic origin of the ozone isotope effect: a critical analysis of enrichments and rate coefficients. *Physical Chemistry Chemical Physics* **2001**, *3*, 4718-4721.

(14) Janssen, C.; Tuzson, B. Isotope Evidence for Ozone Formation on Surfaces. *J. Phys. Chem.* **2010**, *A 114(36),* 9709-9719.

(15) Mauersberger, K.; Krankowsky, D.; Janssen, C. Oxygen Isotope Processes and Transfer Reactions. *Space Science Reviews* **2003**, 106: 265-279.

(16) Feilberg, K.L.; Wiegel, A.A.; Boering K.A. Probing the unusual isotope effects in ozone formation: Bath gas and pressure dependence of the non-mass-dependent isotope enrichments in ozone. *Chemical Physics Letters*, **2013**, 556, 1–8. doi:10.1016/j.cplett.2012.10.038.(28).

(17) Krankowsky, D.; Mauersberger, K. Atmospheric chemistry - Heavy ozone - A difficult puzzle to solve. *Science* **1996**, *274*, 1324-1325.

(18) Gellene, G.I. An explanation for symmetry-induced isotopic fractionation in ozone. *Science* **1996**, *274*, 1344-1346.

(19) Gao, Y.Q.; Marcus, R.A. Strange and unconventional isotope effects in ozone formation. *Science* **2001**, *293*, 259-263.

(20) Gao, Y.Q.; Marcus, R.A. On the theory of the strange and unconventional isotopic effects in ozone formation. *Journal of Chemical Physics* **2002**, *116*, 137-154.

(21) Miklavc, A.; Peyerimhoff, S.D. Rates of formation of ozone isotopomers: a theoretical interpretation. *Chemical Physics Letters* **2002**, *359*, 55-62.

(22) Babikov, D.; Walker, R.B.; Pack, R.T. A quantum symmetry preserving semiclassical method. *Journal of Chemical Physics* **2002**, *117*, 8613-8622.

(23) Baker, T.A.; Gellene, G.I. Classical and quasi-classical trajectory calculations of isotope exchange and ozone formation proceeding through O+O-2 collision complexes. *Journal of Chemical Physics* **2002**, *117*, 7603-7613.

(24) Babikov, D.; Kendrick, B.K.; Walker, R.B.; Pack, R.T.; Fleurat-Lesard, P.; Schinke, R. Formation of ozone: Metastable states and anomalous isotope effect. *Journal of Chemical Physics* **2003**., *119*, 2577-2589.

(25) Fleurat-Lessard, P.; Grebenshchikov, S.Y.; Schinke, R.; Janssen, C.; Krankowsky, D. Isotope dependence of the $O+O_2$ exchange reaction: Experiment and theory *J. Chem. Phys*. **2003**, *119*, 4700.

(26) Marcus, R.A. Mass-independent isotope effect in the earliest processed solids in the solar system: A possible chemical mechanism. *Journal of Chemical Physics* **2004**, *121*, 8201-8211.

(27) Pack, R.T.; Walker, R.B. Some symmetry-induced isotope effects in the kinetics of recombination reactions. *Journal of Chemical Physics* **2004**, *121*, 800-812.

(28) Schinke, R.; Grebenshchikov, S.Y.; Ivanov, M.V.; Fleurat-Lessard, P. Dynamical studies of the ozone isotope effect: A status report, *Annual Review of Physical Chemistry* **2006**, pp. 625-661.

(29) Ivanov, M.V.; Babikov, D. On molecular origin of mass-independent fractionation of oxygen isotopes in the ozone forming recombination reaction. *PNAS* **2013**, *110*, 17708-17713.

(30) Urey, H.C. The thermodynamic properties of isotopic substances. *Journal of the Chemical Society*, **1947**, 562-581.

(31) Bigeleisen, J. The relative reaction velocities of isotopic molecules. *Journal of Chemical Physics* **1949**, *17*, 675-678.

(32) Young, E.D.; Galy, A.; Nagahara, H. Kinetic and equilibrium mass-dependent isotope fractionation laws in nature and their geochemical and cosmochemical significance. *Geochimica and Cosmochimica Acta* **2002**, *66*, 1095-1104.

(33) Reinhardt, P.; Robert, F. Mass independent isotope fractionation in ozone. *Earth and Planetary Science Letters* **2013**, *368*, 195-203.

(34) Reinhardt, P.; Robert, F. On the mass independent isotopic fractionation in ozone. *Chemical Physics*. **2018**. https://doi.org/10.1016/j.chemphys.2018.07.040.

(35) Rao, T.R. ; Guillon, G. ; Mahapatra, S.; Honvault P. Huge Quantum Symmetry Effect in the O + O_2 Exchange Reaction. J. *Phys. Chem. Lett.* **2015**, 6, 633−636. DOI: 10.1021/jz5026257.

(36) Baraut-Guinet, L.; Robert, F.; Cartigny, P. Unconventionnal mass-independent oxygen isotope effect in ozone by microwave discharge plasma. *International Symposium of Isotopomers* **2016**, Nantes, France. DOI: 10.13140/RG.2.2.19709.97761.

(37) Teplukin, A.; Babikov, D. Several Levels of Theory for Description of Isotope Effects in Ozone: Symmetry Effect and Mass Effect. *J.Phys. Chem. A* (in press).

(38) Teplukin, A.; Gayday I.; Babikov, D. Several levels of theory for description of isotope effects in ozone: Effect of resonance lifetimes and channel couplings. *J. Chem. Phys.* **2018**, 149, 164302. doi.org/10.1063/1.5042590.

(39) Schinke, R.; Fleurat-Lessard, P.; Grebenshchikov, S.Y. Isotope dependence of the lifetime of ozone complexes formed in $O+O_2$ collisions. *Physical Chemistry Chemical Physics* **2003**, *5*, 1966-1969.

(40) Schinke, R.; Fleurat-Lessard, P. The effect of zero-point energy differences on the isotope dependence of the formation of ozone : a classical trajectory study. *J. Chem. Phys*. **2005**, *122*, 094317. DOI: 10.1063/1.1860011.

(41) Schinke, R.; Fleurat-Lessard, P.; Grebenshchikov S.Y. Isotope dependence of the lifetime of ozone complexes formed in $O+O_2$ collisions. *Phys. Chem. Chem. Phys*., **2003**, 5, 1966–1969. DOI: 10.1039/b301354e.

(42) Kaufman, F.; Kelso, J.R. M effect in the gas-phase recombination of O with O_2. *J. Chem. Phys*. **1967**, *46*, 4541-4543.

(43) Kaye, J.A.; Strobel, D.F. Enhancement of Heavy Ozone in the Earth's Atmosphere? J. Geophys. Res., **1983**, *88*, 8447-8452.

(44) Marinov D.; Guaitella O.; Booth J.P.; Rousseau A. Direct observation of ozone formation on SiO_2 surfaces in O_2 discharges J. Phys. D: Appl. Phys. ***2013***, *46* 032001.